QUANTITATIVE ANALYSIS OF REACTION GASES OR EXHAUST USING AN ONLINE PROCESS MASS SPECTROMETER

Fu-Qiang Wei[1], Ze-Jian Huang[2], You Jian[2], Xin-Hua Dai[2], Xiang Fang[2], Shang-Zhong Jin[1]

1) *China Jiliang University, College of Optical and Electronic Technology, Hangzhou, Zhejiang 310018 China*
   (*weifuqiang@163.com,* ✉ *jinsz@cjlu.edu.cn*)
2) *National Institute of Metrology, Technology Innovation Center of Mass Spectrum for State Market Regulation, Center for Advanced Measurement Science, Beijing 100029, China*
   (✉ *huangzj@nim.ac.cn, jiangyou@nim.ac.cn, daixh@nim.ac.cn, fangxiang@nim.ac.cn*)

Abstract

Online quantitative analysis of reaction gases or exhaust in industrial production is of great significance to improve the production capacity and process. A novel method is developed for the online quantitative analysis of reaction gases or exhaust using quantitative mathematical models combined with the linear regression algorithm of machine learning. After accurately estimating the component gases and their contents in the reaction gases or exhaust, a ratio matrix is constructed to separate the relevant overlapping peaks. The ratio and calibration standard gases are detected, filtered, normalized, and linearly regressed with an online process mass spectrometer to correct the ratio matrices and obtain the relative sensitivity matrices. A quantitative mathematical model can be established to obtain the content of each component of the reaction gases or exhaust in real time. The maximum quantification error and relative standard deviation of the method are within 0.3% and 1%, after online quantification of the representative yeast fermenter tail gas.

Keywords: online quantitative analysis, mass spectrometers, mathematical models, monitoring.

1. Introduction

Process analytical technologies play an important role in efficient, intelligent, and green industrial production [1,2]. Excellent online quantitative analysis technologies monitor the content of each component of reaction gas or exhaust in real time, and adjust the production process in time for efficient use of energy and optimization and upgrading of products.

The *gas chromatograph* (GC) [3–5] and *mass spectrometer* (MS) [6–8] are common instruments for online quantitative analysis of gases. The analysis speed of gas chromatography is slow and different chromatographic columns are required to detect different substances. Therefore, the gas chromatograph cannot perform simultaneous detection in multiple pipelines. Compared to the

gas chromatograph, the mass spectrometer is faster, and more widely applicable in simultaneous detection of multiple lines containing multiple component gases.

In an actual industrial production process, component gases and approximate contents of reaction gases or exhaust can be deduced. An online mass spectrometer is used to monitor variations in the content of component gases for timely manual intervention or intelligent regulation of the production system to achieve stable production. Most online quantitative analysis methods with mass spectrometers are based on the formulation of the standard gas associated with the reaction gas or exhaust to detect ion abundances and pressures. These calibration parameters are then linearly fitted to establish a mathematical model for the software system to achieve online quantitative analysis of the reaction gas or exhaust [9–15].

Ferreira *et al.* [9] proposed a method to calculate sensitivity for online quantitative analysis. The sensitivity, also known as scale or calibration factor, is the ratio of relevant ion abundance of each standard gas to the corresponding partial pressure. When quantifying the reaction gas or exhaust online, the relevant sensitivity should be used to obtain the partial pressure of each component gas at the corresponding ion abundance. The content of each component gas can then be determined according to the linear relationship between partial pressures. However, this method has a limitation, that is, the bombardment of mixed-composition gases with strong electrons produces not only ions corresponding to various composition gases but also many fragment ions [16]. After mass spectrometer detection, the *mass-to-charge ratio* (m/z) of corresponding ions may produce the base peak, and that of the corresponding fragment can produce the fragment peak. The simultaneous ionization of the molecules of each component gas produces ions, and it is possible that the ion abundances of several component gases may be linearly superimposed at the same mass-to-charge ratio to produce overlapping peaks [17]. This method will not yield accurate results once the selected quantitative ions are related to overlapping peaks.

Kaiser R. *et al.* [10] and Cheng Z. *et al.* [11,12] proposed an improved method for separating overlapping peaks. In this method, the ratio and sensitivity of the fragment peak to the base peak of each component gas are used to construct a system of linear equations for stripping the overlapping peaks. Therefore, the partial pressure of each component gas can be used to calculate its content. However, the changes in the gas pressure can cause the changes in the injection amount, and the obtained sensitivity cannot be adapted to the actual ion abundance, resulting in a large error in the quantification of each component gas.

Velasco-Rozo E.A. *et al.* [13] proposed a method using the sensitivity obtained from the ion abundance normalization value and the partial pressure normalization value of each component gas for online quantitative analysis. Compared to the methods of Kaiser R.I. *et al.* and Cheng Z. *et al.*, this method is only related to the content and ion abundance ratio of each component gas. The sensitivity obtained is more applicable because the content and ion abundance ratio are less affected by pressure fluctuations [18]. However, the mathematical model established is more complex, and the ion abundance and partial pressure normalization are not excluded from the outliers, so the quantitative accuracy is low.

When these three methods are used to quantify any of reaction gases or exhaust, the standard gases corresponding to all their component gases need to be formulated for parameter calibration to complete the quantification, which leads to high quantification costs and workloads. In addition, the partial pressure of each component gas used to calculate the content is excessively dependent on the accuracy and stability of the pressure instruments, and the relevant ion abundance data processing is not fully considered. As a result, the quantification error can only be controlled within 3%, and the relative standard deviation of quantification can only be controlled within 10%.

This research proposes a method to develop quantitative mathematical models with the ratio matrices and relative sensitivity matrices, combined with the linear regression algorithm of machine learning for online quantitative analysis of reaction gases or exhaust. This method

aims to ensure the accurate separation of overlapping peaks. The component gases and their corresponding contents are accurately estimated for the corresponding reaction gas or exhaust, and their relevant overlapping peaks and the ratio matrix are obtained from a library of standard mass spectrums. In addition, the corresponding ratio standard gases and calibration standard gases are formulated and detected with an online process mass spectrometer to obtain the relevant ion abundance curves. These curves are filtered, normalized, and linearly regressed with machine learning to correct the ratio matrix and obtain the relative sensitivity matrix in order to establish a mathematical model for quantitative analysis and monitoring of the reaction gases or exhaust. The proposed method showed high accuracy and applicability when applied to the yeast fermenter tail gas, and the maximum quantitative error is controlled within 0.3% and the maximum relative standard deviation is controlled within 1%.

2. Experimental section

2.1. Instrument structure

The overall structure of the self-developed online process mass spectrometer (Fig. 1) includes two parts: the gas injection system and the detection system. The injection system consists of a reduction valve, an EMT2CSC16MWE multiple directional control valve from Valco Instru-
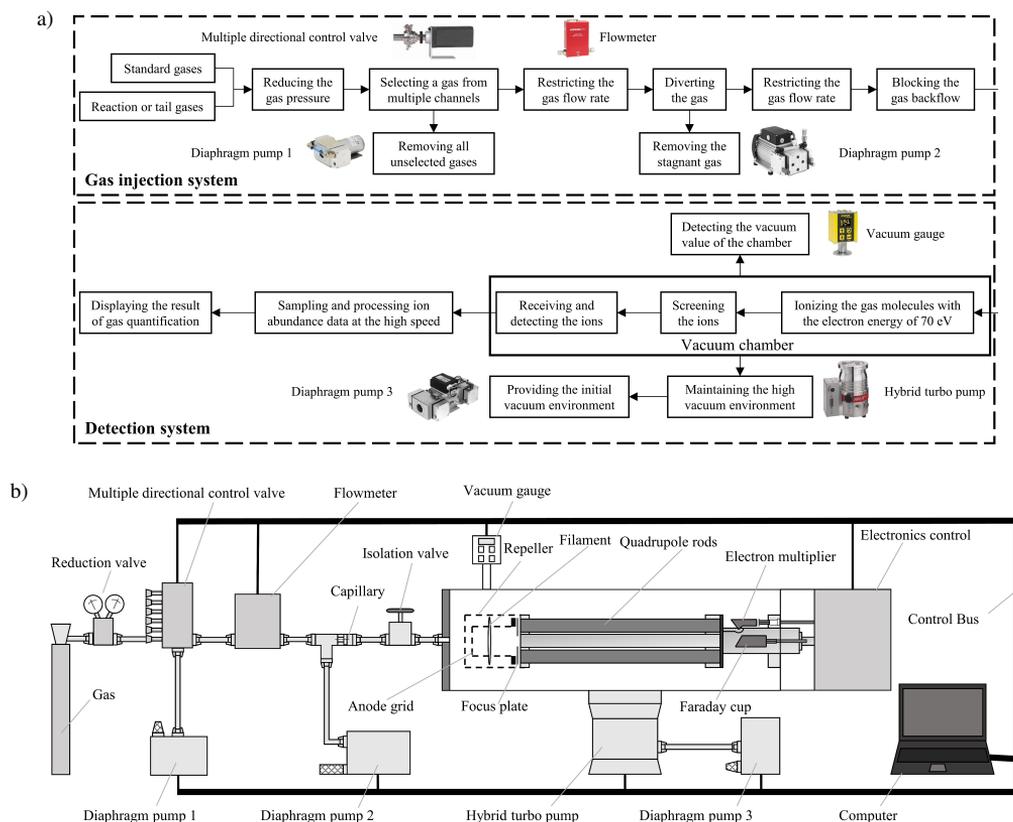

Fig. 1. (a) Workflow of the self-developed online process mass spectrometer. (b) Overall structure of the self-developed online process mass spectrometer.

ments Co. Inc. (Houston, TX, USA), an N84.3ANDC Diaphragm Pump 1 from KNF Neuberger GmbH (Freiburg, Germany), an S48-32 flowmeter from HORIBA (Kyoto, Japan), an MVP015-2 Diaphragm Pump 2 from Pfeiffer Vacuum GmbH (Asslar, Germany), an isolation valve, and self-developed diverter modified from a three-channel connector with the exhaust end connected to the Diaphragm Pump 2 through a pipeline and the inlet end through a capillary (15 mm in length and 0.15 mm in internal diameter) to complete the injection. The detection system consists of a self-developed quadrupole mass spectrometer, an IGM401 vacuum gauge from InstruTech (Longmont, CO, USA), a SplitFlow 80 hybrid turbo pump from Pfeiffer Vacuum GmbH (Asslar, Germany), and an N84.4ANDCB Diaphragm Pump 3 from KNF Neuberger GmbH (Freiburg, Germany).

2.2. Standard gas

The tail gas of a yeast fermenter is used for analysis. Three standard gases are used as background gas, calibration standard gas, and ratio standard gas, all of which are formulated by the Shanghai Material Special Gases Co. Ltd. (Shanghai, China). As water vapor can greatly affect the results of the mass spectrometer detection process, the water vapor is removed from all gases. The background gas is pure He (mol/mol, > 99.999%). The calibration standard gas is formulated as the yeast fermenter tail gas and consists of N_2 (mol/mol, 78%), O_2 (mol/mol, 19%), Ar (mol/mol, 1%), and CO_2 (mol/mol, 2%). The ratio standard gas is formulated according to the overlapping peak of each component gas in the calibration standard gas and consists of CO_2 (mol/mol, 2%) and He (mol/mol, 98%). The upper and lower deviation of the content of each component gas in the calibration standard gas and the ratio standard gas should not exceed 0.05%.

2.3. Experimental condition

Before the gas detection, the vacuum gauge is checked to ensure that the chamber of the mass spectrometer is in a stable high vacuum environment. When the isolation valve is closed, the vacuum value is above 1×10^{-6} Pa. When the isolation valve is opened, the vacuum value slowly decreases to above 1×10^{-4} Pa. When the detection is carried out, the flow rate of the flowmeter and the rotational speed of Diaphragm Pump 2, Diaphragm Pump 3, and hybrid turbo pump are monitored and adjusted by a computer in real time. The injection volume of the gas and the displayed value of the vacuum gauge are maintained at the set value. The final flow rate of the flowmeter is 5 mL/min, and the final value of the vacuum gauge is about 4×10^{-4} Pa. The electron impact ion source with a grid structure is used to ionize the gas molecules at the electron energy of 70 eV. Free hot electrons are generated by the circular filament and accelerated into the anode grid, most of which collide with the gas molecules to produce ions. A small fraction passes through the anode grid and is decelerated and then accelerated into the anode grid again to ionize gas molecules under the electric field of the anode grid and the repeller.

2.4. Effective ion abundance detection

Residual gases may be present in the chambers and pipelines of each online process mass spectrometer, and their generated ion abundances may be linearly superimposed on the ion abundances of the relevant standard gases, which affects the accuracy of the detection results [19, 20]. Therefore, before each detection, the background standard gas should be introduced and the full scan of the mass spectrometer should be turned on to obtain the interfering ion abundances of the relevant mass-to-charge ratio. The mass spectrometer should be switched to the *selected ion monitoring* (SIM) to monitor the changes in the interfering ion abundances. When the interfering

ion abundances remain constant or change within the allowed error range, the average values of the interfering ion abundances of the corresponding end smoothing time periods should be obtained and used to determine the undisturbed effective ion abundances of the relevant standard gas (Eq. (1)).

$$I_{cij} = I_{ij} I_{bij},\tag{1}$$

where I_{cij} is the effective ion abundance of the j-th component gas at the i-th mass-to-charge ratio in the relevant standard gas; I_{ij} is the ion abundance of the j-th component gas at the i-th mass-to-charge ratio in the relevant standard gas; and I_{bij} is the average value of the interfering ion abundance of the j-th component gas at the i-th mass-to-charge ratio in the relevant standard gas.

Before turning on the standard gases, they should be connected to the channels of the multiple directional control valve to further prevent the interfering gases from entering the pipeline and producing the interfering ion abundances. The Diaphragm Pump 1 should be activated to remove all interfering gases from the pipeline. When the multiplexed directional control valve is switched between the standard gases, it is necessary to ensure that the standard gas for the present phase of detection is turned off and with no ion abundance before switching on the next phase of the opened standard gas to be detected.

2.5. Overlapping peak separation

Most of the reaction gases or exhaust for the online quantitative analysis are mixtures of multiple component gases. The detected ion abundances at the relevant mass-to-charge ratios may be overlapping peaks consisting of the corresponding ion abundances of multiple component gases. However, each ion abundance is generated from each corresponding component gas, and the ion species of each component gas is relatively fixed after ionization. Therefore, the ion abundances in the overlapping peaks can be separated by preparing the ratio standard gases with the same content as the corresponding component gases for the detection at the full scan, and obtaining their established ratio of each ion abundance to the base peak (Eq. (2)).

$$\beta_{ij} = \frac{I_{cij}}{I_{cj}} \times 100,\tag{2}$$

where β_{ij} is the established ratio of the j-th component gas at the i-th mass-to-charge ratio in the ratio standard gas; I_{cij} is the effective ion abundance of the j-th component gas at the i-th mass-to-charge ratio in the ratio standard gas; and I_{cj} is the effective highest peak of the j-th component gas in the ratio standard gas, *i.e.*, the base peak.

2.6. Calibrated mathematical model

Once the standard gas enters the mass spectrometer chamber, the original vacuum environment is immediately destroyed. The vacuum gauge returns to the set vacuum value only after a period of automated control. During the fluctuation of the standard gas injection and real-time automated modulation, the ion abundances obtained by the mass spectrometer for the full scan or selected ion monitoring of the standard gases at the relevant mass-to-charge ratios can only be normalized to eliminate the simultaneous fluctuation of each ion abundance during the detection process (Eq. (3)).

$$r_{tij} = \frac{I_{ctij}}{\sum (I_{ctij})},\tag{3}$$

where r_{tij} is the ratio of the effective ion abundance of the j-th component gas at the i-th mass-to-charge ratio to the sum of the effective ion abundances at the t-th moment, *i.e.*, the normalized

value; and I_{ctij} is the effective ion abundance of the j-th component gas at the i-th mass-to-charge ratio of the detected gas at the t-th moment.

After detecting the calibration standard gas and obtaining the normalized values of the effective ion abundances at the corresponding mass-to-charge ratios, the calibrated mathematical model can be established from the linear relationship of the overlapping peaks to calculate the required relative sensitivity matrix. In order to make the relative sensitivity matrix close to the true value, when establishing the calibrated mathematical model, the effective ion abundances with the smoothest normalized value and the sum of its effective ion abundances at each moment should be selected for linear regression to eliminate the outliers and get the linear regression function. The slope of linear regression function should be used as the correction value of the calibrated mathematical model (Eq. (4)).

$$
\begin{cases}
\beta_{11}\varphi_1\alpha_1 + \beta_{12}\varphi_2\alpha_2 + \ldots + \beta_{1j}\varphi_j\alpha_j = \gamma_1 \\
\beta_{21}\varphi_1\alpha_1 + \beta_{22}\varphi_2\alpha_2 + \ldots + \beta_{2j}\varphi_j\alpha_j = \gamma_2 \\
\qquad\qquad\qquad \vdots \\
\beta_{i1}\varphi_1\alpha_1 + \beta_{i2}\varphi_2\alpha_2 + \ldots + \beta_{ij}\varphi_j\alpha_j = \gamma_i
\end{cases} \quad (i = j)
$$

$$
\begin{bmatrix}
\beta_{11} & \beta_{12} & \cdots & \beta_{1j} \\
\beta_{21} & \beta_{22} & \cdots & \beta_{2j} \\
\vdots & \vdots & \vdots & \vdots \\
\beta_{i1} & \beta_{i2} & \cdots & \beta_{ij}
\end{bmatrix}_{i=j}
\begin{bmatrix}
\varphi_1 & 0 & \cdots & 0 \\
0 & \varphi_2 & \ddots & \vdots \\
\vdots & \ddots & \ddots & 0 \\
0 & \cdots & 0 & \varphi_j
\end{bmatrix}
\begin{bmatrix}
\alpha_1 \\ \alpha_2 \\ \vdots \\ \alpha_j
\end{bmatrix}
=
\begin{bmatrix}
\gamma_1 \\ \gamma_2 \\ \vdots \\ \gamma_i
\end{bmatrix} \tag{4}
$$

$$
\boldsymbol{\beta} \cdot \boldsymbol{\varphi} \cdot \boldsymbol{\alpha} = \boldsymbol{\gamma},
$$

where β_{ij} is the established ratio of the j-th component gas in the calibration standard gas at the i-th mass-to-charge ratio, and $\boldsymbol{\beta}$ is the ratio matrix composed of β_{ij}; φ_j is the content of the j-th component gas in the calibration standard gas, and $\boldsymbol{\varphi}$ is the prediction matrix composed of φ_j; α_j is the relative sensitivity of the j-th component gas, and $\boldsymbol{\alpha}$ is the relative sensitivity matrix composed of α_j; γ_i is the correction value of the effective ion abundance of the calibration standard gas at the i-th mass-to-charge ratio, and $\boldsymbol{\gamma}$ is the correction matrix composed of γ_i.

2.7. Quantitative mathematical model

Based on the ratio matrix $\boldsymbol{\beta}$ and the relative sensitivity matrix $\boldsymbol{\alpha}$, the quantitative mathematical model for online quantitative analysis of the reaction gas or exhaust can be established (Eq. (5)).

$$
\begin{cases}
\beta_{11}\alpha_1 x_1 + \beta_{12}\alpha_2 x_2 + \ldots + \beta_{1j}\alpha_j x_j = y_1 \\
\beta_{21}\alpha_1 x_1 + \beta_{22}\alpha_2 x_2 + \ldots + \beta_{2j}\alpha_j x_j = y_2 \\
\qquad\qquad\qquad \vdots \\
\beta_{i1}\alpha_1 x_1 + \beta_{i2}\alpha_2 x_2 + \ldots + \beta_{ij}\alpha_j x_j = y_i
\end{cases} \quad (i = j)
$$

$$
\begin{bmatrix}
\beta_{11} & \beta_{12} & \cdots & \beta_{1j} \\
\beta_{21} & \beta_{22} & \cdots & \beta_{2j} \\
\vdots & \vdots & \vdots & \vdots \\
\beta_{i1} & \beta_{i2} & \cdots & \beta_{ij}
\end{bmatrix}_{i=j}
\begin{bmatrix}
\alpha_1 & 0 & \cdots & 0 \\
0 & \alpha_2 & \ddots & \vdots \\
\vdots & \ddots & \ddots & 0 \\
0 & \cdots & 0 & \alpha_j
\end{bmatrix}
\begin{bmatrix}
x_1 \\ x_2 \\ \vdots \\ x_j
\end{bmatrix}
=
\begin{bmatrix}
y_1 \\ y_2 \\ \vdots \\ y_i
\end{bmatrix}, \tag{5}
$$

$$
\boldsymbol{\beta} \cdot \boldsymbol{\alpha} \cdot \boldsymbol{x} = \boldsymbol{y},
$$

where x_j is the content of the j-th component gas in the actual reaction gas or exhaust, and $\boldsymbol{x}$ is the content matrix composed of x_j; and y_i is the normalized value of the effective ion abundance at the i-th mass-to-charge ratio of the actual reaction gas or exhaust, and $\boldsymbol{y}$ is the detection matrix composed of y_i.

3. Results and discussion

3.1. Obtaining the ratio matrix

Before online quantification of the reaction gas or exhaust, the component gases and their corresponding contents need to be accurately estimated and the calibration gas needs to be formulated. The yeast fermenter tail gas consists of 78% N_2, 19% O_2, 1% Ar and 2% CO_2. The mass spectrums of each component gas can be obtained from the NIST standard mass spectrum library, and the relative ion abundances of the standard mass spectrums and the estimated contents can be used to extrapolate the relative ion abundances of the corresponding calibration standard gas (Eq. (6)), and plot the mass spectrum of the calibration standard gas with overlapping peaks (Fig. 2a), so that the ratio standard gas can be formulated accurately.

$$R_{ij} = \frac{\tau_{ij} \cdot \varphi_j}{\max\left[\sum_j (\tau_{ij} \cdot \varphi_j)\right]} \times 100, \tag{6}$$

where R_{ij} is the extrapolated relative ion abundance of the j-th component gas in the calibration standard gas at the i-th mass-to-charge; φ_j is the content of the j-th component gas in the calibration standard gas; and τ_{ij} is the relative ion abundance in the standard mass spectrum of the j-th component gas in the calibration standard gas at the i-th mass-to-charge ratio.
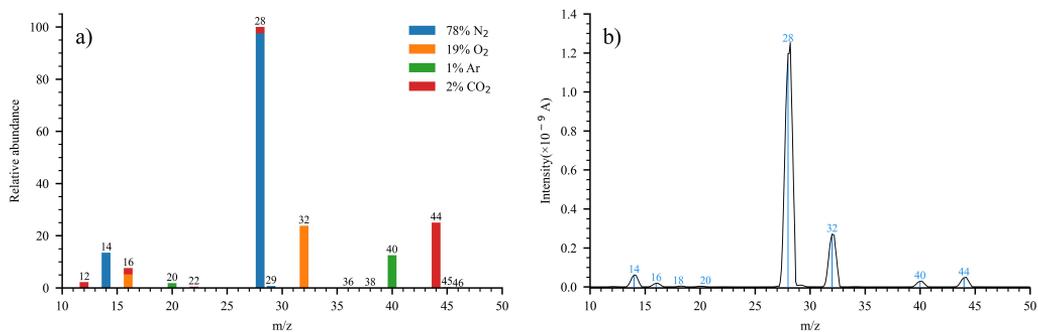

Fig. 2. (a) Extrapolated mass spectrum of calibration standard gas. (b) Actual full scan mass spectrum of the calibration standard gas.

Each bar of the same colour is produced from the component gas with the corresponding content. The base peaks of N_2, O_2, Ar, and CO_2, are respectively at mass-to-charge ratios of 28, 32, 40, and 44. The other smaller bars are the fragment peaks of the four component gases.

The fragment peaks are generally lower, and the base peaks should be preferred when constructing the ratio matrix. If the base peaks of different component gases overlap, then multiple fragment peaks with higher effective ion abundance and less overlap besides the base peaks should be added until the number of component gases is the same as the number of effective ion

www.czasopisma.pan.pl   PAN   www.journals.pan.pl
POLSKA AKADEMIA NAUK

F.-Q. Wei et al.: QUANTITATIVE ANALYSIS OF REACTION GASES OR EXHAUST USING AN ONLINE PROCESS...

abundances corresponding to the selected mass-to-charge ratio, *i.e.*, the equation of "$i = j$" in Eqs. (4) and (5). Given the differences in the online process mass spectrometer and the experimental environment, the actual detected mass spectrum of the calibration standard gas may differ from the extrapolated mass spectrum obtained from the standard mass spectrum library (Fig. 2).

Therefore, after examining the actual full-scan mass spectrum of the calibration standard gas and the extrapolated mass spectrum, with the assistance of Eq. (2), an accurate ratio matrix $\boldsymbol{\beta}_s$ can be constructed (Eq. (7)).

$$\boldsymbol{\beta}_s = \begin{bmatrix} 100 & 0 & 0 & 9.8 \\ 0 & 100 & 0 & 0 \\ 0 & 0 & 100 & 0 \\ 0 & 0 & 0 & 100 \end{bmatrix}, \tag{7}$$

where each row of the ratio matrix $\boldsymbol{\beta}_s$ represents the established ratio of each component gas in the calibration standard gas at mass-to-charge ratios 28, 32, 40, and 44; and each column represents the established ratio of N_2, O_2, Ar, and CO_2 in the calibration standard gas at each mass-to-charge ratio.

3.2. Correcting the ratio matrix

The ratio in the ratio matrix $\boldsymbol{\beta}_s$ is only the established ratio calculated from the NIST standard mass spectrum library, which may be inaccurate compared to the actual ratio. As such, the ratio standard gas should be formulated with the same content as the corresponding component gas in the calibration standard gas to correct the ratio matrix $\boldsymbol{\beta}_s$. From Eq. (6), the ratio matrix $\boldsymbol{\beta}_s$ shows that the base peak of N_2 and the fragment peak of CO_2 overlap only at a mass-to-charge ratio of 28. Therefore, the base peak of N_2 can be separated more accurately when only the ratio standard gas consisting of 2% CO_2 and 98% He is formulated to correct the established ratio of CO_2 at the mass-to-charge ratio of 28.

When the online process mass spectrometer performs high speed detection of the ratio standard gas for a limited long time, it is subject to various types of noise interference. Many burrs may appear on the effective ion abundance curves, making the true effective ion abundance drown in the burrs. Generally, the true effective ion abundance for a limited long time is mostly distributed in the low frequency band, and the burrs are mostly distributed in the high frequency band. Therefore, the low-pass filter is considered to smoothen the detected effective ion abundance curves.

In order to obtain better filtration and to facilitate the application, it is considered to use the Savitzky–Golay filter [21], which is the least-squares fitting of the selected data region through the active window to remove the outliers in the time domain, with different filtering effects obtained from the adjustment of the size of the active window and the order of the fitting polynomial. Since the least squares method for fitting the data requires solving the inverse matrix of the corresponding data, but there is the possibility that the inverse matrix is not available in the actual data, the gradient descent algorithm of machine learning is used to improve the least-squares fitting in the Savitzky–Golay filter. The differences and distortions of the effective ion abundance curves before and after the filtering are evaluated with the mean square error ratio and the relative standard deviation ratio to ensure the true effective ion abundances without large distortions for more accurate quantitative results.

After multiple adjustments, it is demonstrated that for the effective ion abundance curves at mass-to-charge ratios of 28 and 44 for the ratio standard gas, the mean square error ratio before

and after the filter should be below 0.3 and the relative standard deviation ratio should be above 0.4. Therefore, a Savitzky–Golay filter with a window size of 65 and a fitting order of 1 can be chosen for smoothing (Figs. 3a and 3b).
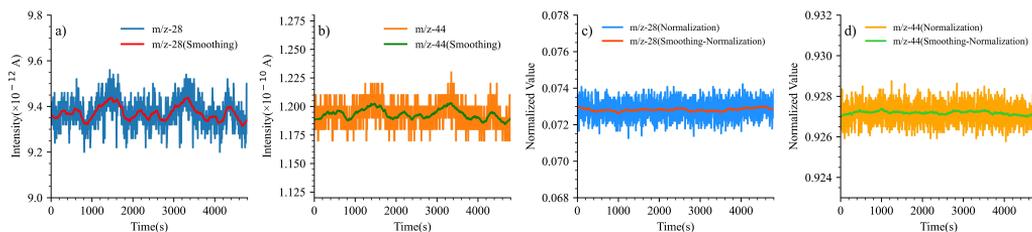

Fig. 3. Detection and treatment of the ratio standard gas.

The variations in the environment and the automatic adjustment of the gas injection system may change the content of each component gas, resulting in the changes in the ratio between the effective ion abundances, which can be normalized with Eq. (3) to monitor the changes in the content of each component gas in real time. The whole normalized curves at mass-to-charge ratios of 28 and 44 are relatively flat (Figs. 3c and 3d). Hence, the established ratios between the effective ion abundances never change significantly. The fluctuations of the effective ion abundances are mostly related to the injection volume (Figs. 3a and 3b), and neither does the content of each component gas change clearly. However, the linear regression algorithm of machine learning can be performed on all smoothed effective ion abundances at mass-to-charge ratios of 28 and 44 (Fig. 4) to remove the outliers and accurately correct the established ratio of CO_2 at mass-to-charge ratio of 28. The slope of the linear regression function is used to correct the established ratio of CO_2 at the mass-to-charge ratio of 28 to obtain the ratio matrix β_{su} (Eq. (8)).

$$\beta_{su} = \begin{bmatrix} 100 & 0 & 0 & 6.63 \\ 0 & 100 & 0 & 0 \\ 0 & 0 & 100 & 0 \\ 0 & 0 & 0 & 100 \end{bmatrix}. \tag{8}$$
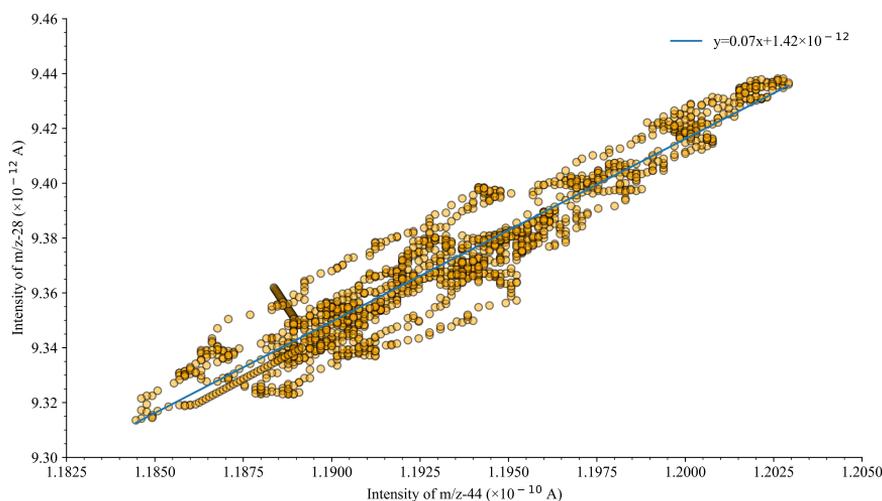

Fig. 4. Linear regression of smoothed effective ion abundances of the ratio standard gas.

3.3. Calculating the relative sensitivity matrix

The calibration mathematical model of Eq. (4) and the quantitative mathematical model of Eq. (5) show that once the ratio matrix $\boldsymbol{\beta}_s$ is constructed, the effective ion abundances to be detected for the calibration standard gas and the yeast fermenter tail gas are determined; that is, the effective ion abundances at mass-to-charge ratios of 28, 32, 40, and 44.

When the online process mass spectrometer is used to detect the calibration standard gas at high speed for a limited long time, the corresponding effective ion abundance curves are subject to different levels of noise interference because of the differences in the content of each component gas, and different Savitzky–Golay filters need to be selected for smoothing separately. After the repeated adjustment, for the effective ion abundance curves at the mass-to-charge ratios of 28, 32, 40 and 44, the mean square error ratio should be below 0.6 and the relative standard deviation ratio should be above 0.6 before and after the filtering. Therefore, different Savitzky–Golay filters with window sizes of 71, 15, 61 and 31, respectively, and all fitting orders of 1 are selected correspondingly for smoothing (Figs. 5a to 5d).
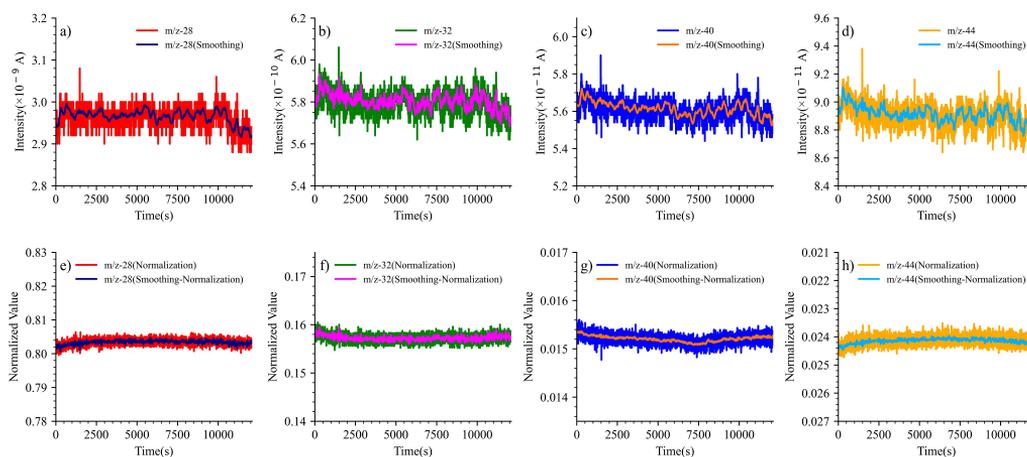

Fig. 5. Detection and treatment of the calibration standard gas.

As shown in the normalized curves (Figs. 5e to 5h), the content of each component gas of the calibration standard gas never changes obviously, so the whole smoothed effective ion abundances can be further processed to reject the outliers. Each effective ion abundance and the sum of its effective ion abundances can then be processed with the linear regression algorithm of machine learning (Figs. 6a to 6d). The correction matrix $\boldsymbol{\gamma}_{su}$ can be constructed with the slopes of each
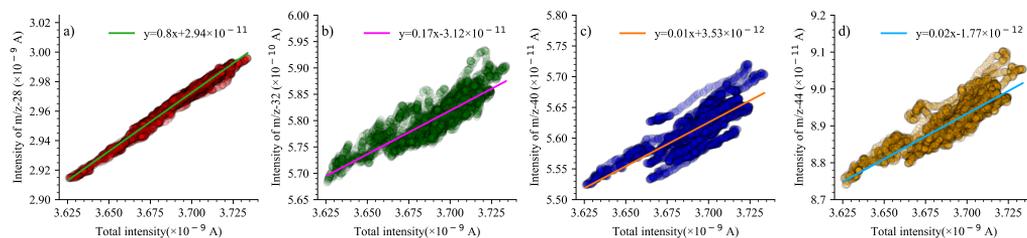

Fig. 6. Linear regression of smoothed effective ion abundance of the calibration standard gas.

linear regression function (Eq. (9)).

$$\boldsymbol{\gamma}_{su} = \begin{bmatrix} 0.79543782 \\ 0.16569273 \\ 0.01424893 \\ 0.02462052 \end{bmatrix}. \tag{9}$$

The relative sensitivity matrix $\boldsymbol{\alpha}_{su}$ can be obtained according to the correction mathematical model (Eq. (10)).

$$\left[\boldsymbol{\beta}_{su} \cdot \boldsymbol{\varphi} \right]^{-1} \cdot \boldsymbol{\gamma}_{su} = \boldsymbol{\alpha}_{su} = \begin{bmatrix} 1.0177 \times 10^{-4} \\ 8.7207 \times 10^{-5} \\ 1.4249 \times 10^{-4} \\ 1.2310 \times 10^{-4} \end{bmatrix}. \tag{10}$$

3.4. Online quantitative analysis

This work then verifies the accuracy and applicability of the quantitative mathematical model established with the calculated ratio matrix $\boldsymbol{\beta}_{su}$ and relative sensitivity matrix $\boldsymbol{\alpha}_{su}$. The calibration standard gas with the known content of each component gas is used for gas analysis in the validation experiment. For the real reflection of the change content of each component gas, the effective ion abundance curves (Figs. 7a to 7d) are no longer smoothed and linearly regressed but are only normalized (Figs. 7e to 7h). Based on the detection matrix $\boldsymbol{y}_{tsu}$, which is composed of the normalized values of the effective ion abundances at each moment, the quantitative mathematical model of Eq. (5) is solved to obtain the content matrix $\boldsymbol{x}_{tsu}$ of each component gas (Eq. (11)).

$$\left[\boldsymbol{\beta}_{su} \cdot \left(\boldsymbol{e} \cdot \boldsymbol{\alpha}_{su}^{\mathrm{T}} \cdot \boldsymbol{E}_4 \right) \right]^{-1} \cdot \boldsymbol{y}_{tsu} = \boldsymbol{x}_{tsu}, \tag{11}$$

where $\boldsymbol{e}$ is the 4×1 all-ones matrix; $\boldsymbol{E}_4$ is the fourth order identity matrix.
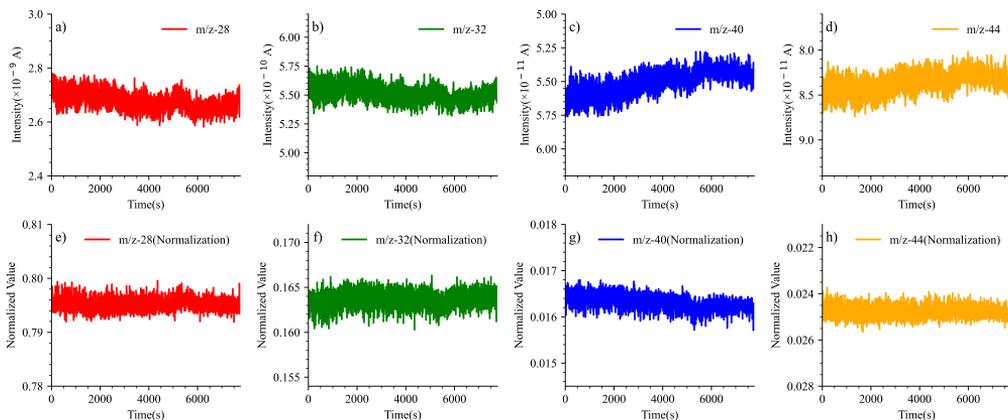

Fig. 7. Detection and normalization of the validation gas.

The content curve is plotted in real time to monitor changes in the content of each component gas (Figs. 8a to 8d). Compared to the real content of each component gas of the calibration standard gas, the actual calculated content of component gas fluctuates within an acceptably small range.

This finding demonstrates the feasibility of the ratio matrix and the relative sensitivity matrix for online quantitative analysis of reaction gases or exhaust.
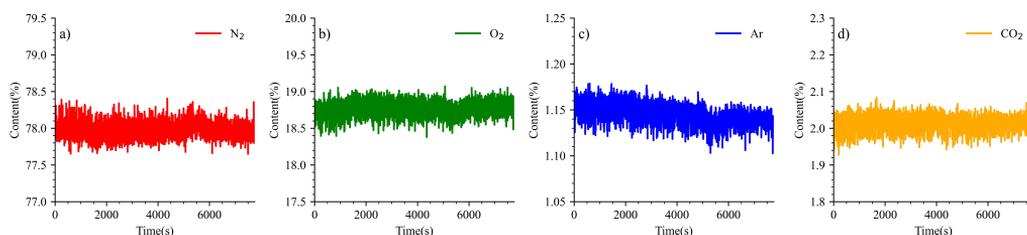

Fig. 8. Online quantitative analysis of the validation gas.

3.5. Method evaluation

Validation experiments were conducted for multiple batches at different times with the calibration standard gas for the more objective evaluation of the accuracy and applicability of the online quantitative analysis method. The accuracy of the method can thus be verified by calculating the average value of each content curve for each batch for the whole time period and comparing it to the real content (Figs. 9a to 9d).
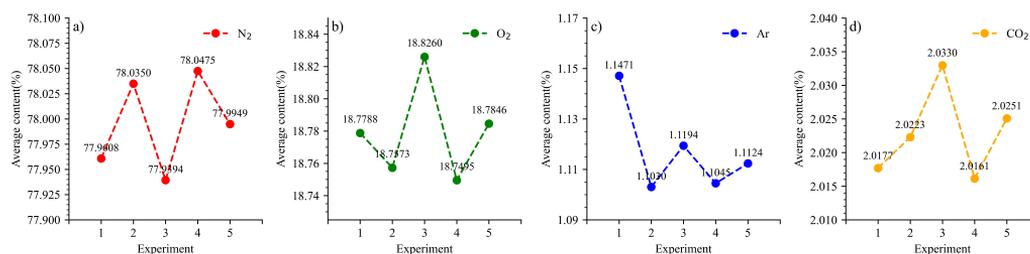

Fig. 9. Variations in the average content of each component gas in multiple batches of validation experiments.

The applicability of the method can be verified through the calculation of the relative standard deviation of the content curves of each batch for the whole time period to reflect the fluctuation of the curves (Figs. 10a to 10d).
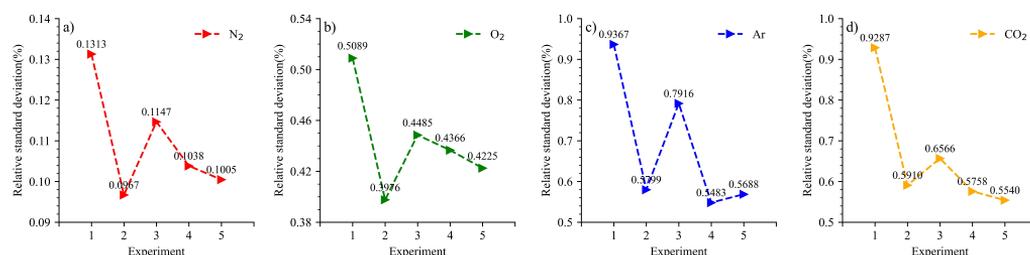

Fig. 10. Variations in the relative standard deviation of each component gas for multiple batches of validation experiments.

Compared to the actual content of each component gas of the calibration standard gas, the average content of O_2 in the validation experiment of Batch 4 differs the most from the actual value,

with the maximum error of 0.2505% (Fig. 9b). Comparison of the relative standard deviations of the component gases in each batch showed that the largest relative standard deviation is 0.9367% for Ar in the validation experiment of Batch 1 (Fig. 10c).

4. Conclusions

This research has developed a method to separate overlapping peaks of the reaction gas or exhaust and quantify their component gases using a quantitative mathematical model based on a ratio matrix and a relative sensitivity matrix, combined with the linear regression algorithm of machine learning. This method is not only accurate, but also applicable. For online quantitative analysis of the representative yeast fermenter tail gas, the maximum quantification error is within 0.3% and the maximum quantification relative standard deviation is within 1%. When the scenarios for online quantitative analysis are changed, this method is still applicable. Whenever the component gases and their contents of the relevant reaction gases or exhaust can be accurately estimated on the basis of the principles of this method, and the corresponding standard gas can be formulated. The applicable calibration mathematical model and quantitative mathematical model can be constructed for the online quantitative analysis of the corresponding reaction gas or exhaust. The application of this method to the online quantification and real-time monitoring of the reaction gases or exhaust in the industrial production process can improve the production capacity and optimize the products through timely adjustment of the industrial production when the contents of each component gas change abnormally.

References

[1] Chew, W. & Sharratt, P. (2010). Trends in process analytical technology. *Analytical Methods*, *2*(10), 1412. https://doi.org/10.1039/c0ay00257g

[2] Simon, L. L., Pataki, H., Marosi, G., Meemken, F., Hungerbühler, K., Baiker, A., & Chiu, M. (2015). Assessment of Recent Process Analytical Technology (PAT) Trends: A Multiauthor Review. *Organic Process Research & Development*, *19*(1), 3–62. https://doi.org/10.1021/op500261y

[3] Andersson, R., Boutonnet, M, & Järås, S. (2012). On-line gas chromatographic analysis of higher alcohol synthesis products from syngas. *Journal of Chromatography a*, *1247*, 134–145. https://doi.org/10.1016/j.chroma.2012.05.060

[4] Fan, J., Fu, C., Yin, H., Wang, Y., & Jiang, Q. (2020). Power transformer condition assessment based on online monitor with SOFC chromatographic detector. *International Journal of Electrical Power & Energy Systems*, *118*, 105805. https://doi.org/10.1016/j.ijepes.2019.105805

[5] Sandoval-Bohorquez, V. S., Rozo, E. A. V., & Baldovino-Medrano, V. G. (2020). A method for the highly accurate quantification of gas streams by on-line chromatography. *Journal of Chromatography a*, *1626*, 461355. https://doi.org/10.1016/j.chroma.2020.461355

[6] Bristow, T. W. T., Ray, A. D., O'Kearney-McMullan, A., Lim, L., McCullough, B., & Zammataro, A. (2014). On-line Monitoring of Continuous Flow Chemical Synthesis Using a Portable, Small

Footprint Mass Spectrometer. *Journal of the American Society for Mass Spectrometry*, *25*(10), 1794–1802. https://doi.org/10.1007/s13361-014-0957-1

[7] Holmes, N., Akien, G. R., Savage, R. J. D., Stanetty, C., Baxendale, I. R., Blacker, A. J., & Bourne, R. A. (2016). Online quantitative mass spectrometry for the rapid adaptive optimisation of automated flow reactors. *Reaction Chemistry & Engineering*, *1*(1), 96–100. https://doi.org/10.1039/C5RE00083A

[8] Ray, A., Bristow, T., Whitmore, C., & Mosely, J. (2018). On-line reaction monitoring by mass spectrometry, modern approaches for the analysis of chemical reactions. *Mass Spectrometry Reviews*, *37*(4), 565–579. https://doi.org/10.1002/mas.21539

[9] Ferreira, B. S., Van Keulen, F., & Da Fonseca, M. M. R. (1998). Novel calibration method for mass spectrometers for on-line gas analysis. Set-up for the monitoring of a bacterial fermentation. *Bioprocess Engineering* (Berlin, West), *19*(4), 289–296. https://doi.org/10.1007/s004490050522

[10] Kaiser, R. I., Jansen, P., Petersen, K., & Roessler, K. (1995). On line and in situ quantification of gas mixtures by matrix interval algebra assisted quadrupole mass spectrometry. *Review of Scientific Instruments*, *66*(11), 5226–5231. https://doi.org/10.1063/1.1146089

[11] Cheng, Z., Mozammel, T., Patel, J., Lee, W. J., Huang, S., Lim, S., & Li, C. E. (2018). A method for the quantitative analysis of gaseous mixtures by online mass spectrometry. *International Journal of Mass Spectrometry*, 434, 23–28. https://doi.org/10.1016/j.ijms.2018.09.002

[12] Cheng, Z., Lippi, R., Li, C. E., Yang, Y., Tang, L., Huang, S., & Patel, J. (2019). An Experimental and Kinetic Study of the Direct Synthesis of Hydrogen Peroxide from Hydrogen and Oxygen over Palladium Catalysts. *Industrial & Engineering Chemistry Research*, *58*(45), 20573–20584. https://doi.org/10.1021/acs.iecr.9b04177

[13] Velasco-Rozo, E. A., Ballesteros-Rueda, L. M., & Baldovino-Medrano, V. G. (2021). A Method for the Accurate Quantification of Gas Streams by Online Mass Spectrometry. *Journal of the American Society for Mass Spectrometry*, *32*(8), 2135–2143. https://doi.org/10.1021/jasms.1c00090

[14] Giannoukos, S., Antony Joseph, M. J., & Taylor, S. (2017). Portable mass spectrometry for the direct analysis and quantification of volatile halogenated hydrocarbons in the gas phase. *Analytical Methods*, *9*(6), 910–920. https://doi.org/10.1039/C6AY03257E

[15] Li, F., Wang, C., Zhang, Y., He, X., Zhang, C., & Sha, F. (2022). Accurate Concentration Measurement Model of Multicomponent Mixed Gases during a Mine Disaster Period. *ACS Omega*, *7*(29), 25443–25457. https://doi.org/10.1021/acsomega.2c02391

[16] Watson, J. T. & Sparkman, O. D. (2007). *Introduction to Mass Spectrometry: Instrumentation, Applications, and Strategies for Data Interpretation* (4th ed.). Chichester, West Sussex: John Wiley & Sons Ltd.

[17] Batey, J. H. (2014). The physics and technology of quadrupole mass spectrometers. *Vacuum*, *101*, 410–415. https://doi.org/10.1016/j.vacuum.2013.05.005

[18] Heinzle, E., Moes, J., Griot, M., Kramer, H., Dunn, I. J., & Bourne, J. R. (1984). On-line mass spectrometry in fermentation. *Analytica Chimica Acta*, 163, 219–229. https://doi.org/10.1016/S0003-2670(00)81510-X

[19] Cook, K. D., Bennett, K. H., & Haddix, M. L. (1999). On-Line Mass Spectrometry: A Faster Route to Process Monitoring and Control. *Industrial & Engineering Chemistry Research*, *38*(4), 1192–1204. https://doi.org/10.1021/ie9707984

[20] Heinzle, E., Oeggerli, A., & Dettwiler, B. (1990). On-line fermentation gas analysis: Error analysis and application of mass spectrometry. *Analytica Chimica Acta*, *238*, 101–115. https://doi.org/10.1016/S0003-2670(00)80528-0

[21] Savitzky, A., & Golay, M. J. E. (1964). Smoothing and Differentiation of Data by Simplified Least Squares Procedures. *Analytical Chemistry*, *36*(8), 1627–1639. https://doi.org/10.1021/ac60214a047

Fu-Qiang Wei is currently an M.Sc. student at China Jiliang University. His current research interests include mass spectrometry, mechatronics, signal and information processing, and artificial intelligence technologies.

Xin-Hua Dai obtained the Ph.D. degree from the Institute of Chemistry of the Chinese Academy of Sciences in 2004. She is now a senior researcher, Vice President of the National Institute of Metrology, P.R. China, Chairman of the National Biometrology Technology Committee, Vice Chairman of the National New Materials and Nanometrology Technology Committee. She has authored or coauthored over 100 journal articles. She has won the second prize of the National Science and Technology Progress Award three times. Her current research interests include life science metrology, mass spectrometry technology, and metrology technology management.

Ze-Jian Huang obtained the M. Sc. degree in measurement technology and instruments from Jilin University, China, in 2004. He is currently a senior researcher of the National Institute of Metrology, P.R. China. He holds 22 issued Chinese invention patents and 2 issued US patents. His current interests focus on miniaturization of mass spectrometers and online mass spectrometry technology.

Xiang Fang is currently a senior researcher, President of the National Institute of Metrology, P.R. China, and executive committee of Asia Pacific Metrology Programme (APMP). He has authored or coauthored over 50 journals. He holds 32 issued patents, and has won the second prize of the National Science and Technology Progress Award twice. His current research interests include chemistry, biometric measurement, theoretical study of mass spectrometry and instrument engineering technology.

You Jiang obtained his Ph.D. degree from Jilin University in 2008. He is now a research professor at the National Institute of Metrology, P.R. China, also the director of the Laboratory of Mass Spectrometry. He has authored over 30 journal papers and is currently holding 20 issued patents. He has twice won the second prize of the National Science and Technology Progress Award. His current research interests include chemical & biometrical measurements, mass spectrometry principles and instrumental engineering with main focus on control technologies.

Shang-Zhong Jin obtained his Ph.D. degree from Zhejiang University, and is a professor in the College of Optics and Electronic Technology, China Jiliang University. His research interests include optics, spectroscopy, instrumentation, and metrology.